J. Membrane Biol. 166, 91–100 (1998)

The Journal of
Membrane
Biology

Evidence for a Multi-ion Pore Behavior in the Plant Potassium Channel KAT1

B. Lacombe, J.-B. Thibaud

Laboratoire de Biochimie et Physiologie Moléculaire des Plantes, UM2/INRA/Agro-M/CNRS URA 2133, Place Viala, 34060 Montpellier cedex 1, France

Received: 9 February 1998/Revised: 28 July 1998

Abstract. KAT1 is a cloned voltage-gated K^+ channel from the plant *Arabidopsis thaliana* L., which displays an inward rectification reminiscent of 'anomalous' rectification of the i_f pacemaker current recorded in animal cells. Macroscopic conductance of KAT1 expressed in *Xenopus* oocytes was 5-fold less in pure Rb^+ solution than in pure K^+ solution, and negligible in pure Na^+ solution. Experiments in different K^+/Na^+ or K^+/Rb^+ mixtures revealed deviations from the principle of independence and notably two anomalous effects of the K^+/Rb^+ mole fraction (i.e., the ratio $[K^+]/([K^+]+[Rb^+])$). First, the KAT1 deactivation time constant was both voltage- and mole fraction-dependent (a so-called 'foot in the door' effect was thus observed in KAT1 channel). Second, when plotted against the K^+/Rb^+ mole fraction, KAT1 conductance values passed through a minimum. This minimum is more important for two pore mutants of KAT1 (T259S and T260S) that displayed an increase in P_{Rb}/P_K. These results are consistent with the idea that KAT1 conduction requires several ions to be present simultaneously within the pore. Therefore, this atypical 'green' member of the Shaker superfamily of K^+ channels further shows itself to be an interesting model as well for permeation as for gating mechanism studies.

Key words: Rubidium — anomalous mole fraction effect — foot in the door — channel deactivation — permeation — *Arabidopsis thaliana*

Introduction

For some channels, the analysis of conductance of two permeant ions reveals that the conductance passes through a minimum instead of displaying a monotonic variation as a function of the mole fraction. This phenomenon is known as the *A*nomalous *M*ole *F*raction *E*ffect (AMFE) (*see* Hille, 1992; Aidley & Stanfield, 1996). Analyses of such effects have led to different permeation models (Hille, 1975; Hille & Schwarz, 1978; Wagoner & Oxford, 1987; Shumaker & MacKinnon, 1990; Mironov, 1992; Armstrong & Neyton, 1992; Miller, 1996; Dang & McCleskey, 1998; Kiss et al., 1998; Lester & Dougherty, 1998; Nonner, Chen & Eisenberg, 1998). In combination with results of mutagenesis (especially in the P-domain), these models help in understanding structural and functional relationships of the permeation pathway (Yool & Schwarz, 1996). A multi-ion single-file conduction scheme is the common feature of most of these models (but see for example the model of Nonner et al. (1998) in which the multi-on single-file conduction is not necessary to explain AMFE). Finally, it is worth noting that the very first structural data following the crystallization of the pore region of a K^+ channel (KcsA) led to the demonstration of the multi-ion single-file occupancy (Doyle et al., 1998).

The multi-ion nature of many animal ion channels has been proposed for: K^+ channels (Hagiwara & Takahashi, 1974; Hagiwara et al., 1977; Hille & Schwarz, 1978; Eisenman, Latorre & Miller, 1986; Begenisich & Smith, 1984; Heginbotham & MacKinnon, 1993; Pérez-Cornejo & Begenisich, 1994; Wollmuth, 1995; Stampe & Begenisich, 1996; Mienville & Clay, 1997), Ca^{2+} channels (Hess & Tsien, 1984; Campbell, Rasmusson & Strauss, 1988; Friel & Tsien, 1989; Yang et al., 1993), Na^+ channels (Cahalan & Begenisich, 1976) and Cl^- channels (Tabcharani et al., 1993).

For plant ion channels, AMFE was shown for native K^+ channels located on the plasma membrane of *Chara corallina* (Tester, 1988) and on cytoplasmic droplets of *Nitella* (Draber, Schultze & Hansen, 1991).

The voltage-gated plant K^+ channels cloned and characterized so far (Chérel et al., 1996) display some

Correspondence to: B. Lacombe

hallmarks of the *Shaker* superfamily of K^+ channels (Schroeder, Ward & Gassman, 1994; Jan & Jan, 1997), having six putative transmembrane segments (S1 to S6), including a highly charged S4 segment (believed to be a voltage-sensor), and, between S5 and S6, the highly conserved P (or H5) domain assumed to form part of the pore. As with their animal counterparts, those 'green' members of the Shaker superfamily have been found to assemble as tetramers of the α-subunits (Daram et al., 1997); as well, heterotetramers may assemble in vivo (Dreyer et al., 1997). The plant K^+ channel, KAT1, cloned by functional complementation of a yeast mutant defective in K^+ uptake (Anderson et al., 1992), was the first plant potassium channel that could be expressed and characterized in *Xenopus* oocytes (Schachtman et al., 1992; Véry et al., 1994; Hedrich et al., 1995; Hoshi, 1995; Véry et al., 1995) and then in other expression systems (yeast, Bertl et al., 1995; and *Sf9* insect cell line, Marten et al., 1996). A striking feature of this channel is its inward rectification of current, reminiscent of that of the recently cloned (Santoro et al., 1997, 1998) 'i_f' pacemaker channel (Mayer & Westbrook, 1983; DiFrancesco et al., 1986; McCormick & Pape, 1990).

Saturation of KAT1 conductance was shown with increasing external K^+ concentration (Hedrich et al., 1995; Hoshi, 1995; Véry et al., 1995). This deviation from the independence principle (Hodgkin & Huxley, 1952) indicates that binding interactions occur between conducting ions and the pore. A voltage-dependent Cs^+ block of KAT1 has been reported (Véry et al., 1994; Hedrich et al., 1995; Véry et al., 1995) providing further support for the idea that ions can bind to the pore. Furthermore, the relative distance of the Cs^+ binding site across the electrical field (Woodhull, 1973) depended on K^+ concentration and exceeded unity in some conditions; this suggested that more than one ion may be present simultaneously within the pore and that some competition between K^+ and Cs^+ binding may occur (Becker et al., 1996).

The hypothesis of KAT1 multi-ion occupancy is investigated further in the present paper. Mixtures of K^+ and Rb^+ were used to demonstrate that AMFE is evident in wild-type KAT1 ($G_{Rb}/G_K \approx 0.2$, Véry et al., 1995; Uozumi et al., 1995), and even more pronounced in T259S and T260S mutants ($G_{Rb}/G_K \approx 0.6$, Becker et al., 1996).

Materials and Methods

Preparation of *Xenopus* Oocytes

In vitro cRNA synthesis and oocyte injection were performed as described in Véry et al. (1995). Briefly, oocytes obtained surgically from anesthetized *Xenopus* were defolliculated by a 1 hr collagenase-treatment (1 mg·ml^{-1}, type IA, Sigma Chemical, Saint-Louis, MO) in a medium containing (in mM): 82.5 NaCl, 2 KCl, 1 $MgCl_2$, 5 HEPES-NaOH (pH 7.4). Stage V and VI oocytes were selected and placed in a medium containing in mM: 96 NaCl, 2 KCl, 1.8 $MgCl_2$, 1 $CaCl_2$, 2.5 Na-pyruvate, 5 HEPES-NaOH (pH 7.4) supplemented with 50 mg·ml^{-1} gentamicin. Oocytes were injected with 30 ng of KAT1 cRNA in 50 nl sterile water. Control oocytes were injected with 50 nl of deionized water.

Electrophysiology

Whole-cell currents were recorded using the two-electrode voltage-clamp technique, 3 to 7 days after injection. During recording, oocytes were continuously perfused with bath solution containing (in mM): 100 of KCl + XCl (X being either Na^+ or Rb^+), 1.8 $CaCl_2$, 1 $MgCl_2$, 5 HEPES-NaOH (pH 7.4). All experiments were performed at room temperature (20–22°C). Current-passing and voltage-recording electrodes were filled with 3 M KCl and had tip resistances of 0.5 to 1.5 MΩ and 1 to 2 MΩ respectively in 100 mM KCl. Correction was made for voltage drop through the series resistance to ground (through the bath and the reference electrode) by using a voltage-recording microelectrode in the bath close to the oocyte; the potential of this bath electrode was subtracted from the one of intracellular electrodes in the amplifier, allowing a real-time correction of series resistance to ground. The voltage-clamp amplifier was an Axoclamp 2A (Axon Instruments, Foster City, CA) interfaced with a TL1 DMA Interface (Axon Instruments) to a IBM PC-compatible computer. Voltage-pulse protocol application (*see* Fig. 1*A*, left), data acquisition and data analyses were performed using pClamp (Axon Instruments) and Sigmaplot (Jandel Scientific, Erkrath, Germany). A linear component was subtracted from the recorded data to correct for leak current.

All chemicals were purchased from Sigma Chemical, except for RbCl, which was from Merck (Darmstadt, Germany).

Steady-state Current Analysis

The following expression of the current carried by two permeant monovalent cations (K^+ and X^+) can be derived from the Goldman-Hodgkin-Katz (GHK) model:

$$I_{GHK} = A.E.F.[(P_K \cdot K_e^+ + P_X.X_e^+) - \exp(A.E.) \cdot (P_K \cdot K_i^+ + P_X \cdot X_i^+)]/ [1 - \exp(A.E.)] \quad (1)$$

where, A is $F/(R.T)$, F, R and T having their usual meaning, E is the membrane potential, and where K_e^+ and X_e^+ (resp. K_i^+ and X_i^+) are the external (resp. internal) K^+ and X^+ concentrations, and P_K and P_X are the absolute permeability for K^+ and X^+.

From the Goldman equation for reversal potential (E_{rev}),

$$P_K \cdot K_i^+ + P_X \cdot X_i^+ = (P_K \cdot K_e^+ + P_X \cdot X_e^+) \cdot (\exp(-E_{rev} \cdot A)) \quad (2)$$

Combining Eq. 1 and Eq. 2, yields:

$$I_{GHK} = E.F.A.[P_K \cdot K_e^+ + P_X \cdot X_e^+] \cdot [1 - \exp(A.(E - E_{rev}))]/[1 - \exp(A.E)] \quad (3)$$

When E tends towards $-\infty$ the 2 last terms tend towards 1 and I_{GHK} tends towards:

$$I_{-\infty} = E.F.A.(P_K \cdot K_e^+ + P_X \cdot X_e^+) = E.G_l \quad (4)$$

where G_l is the so-called 'limit inward conductance' (Véry et al., 1995). In other words, the graphic representation of Eq. 3 is a curve that, at

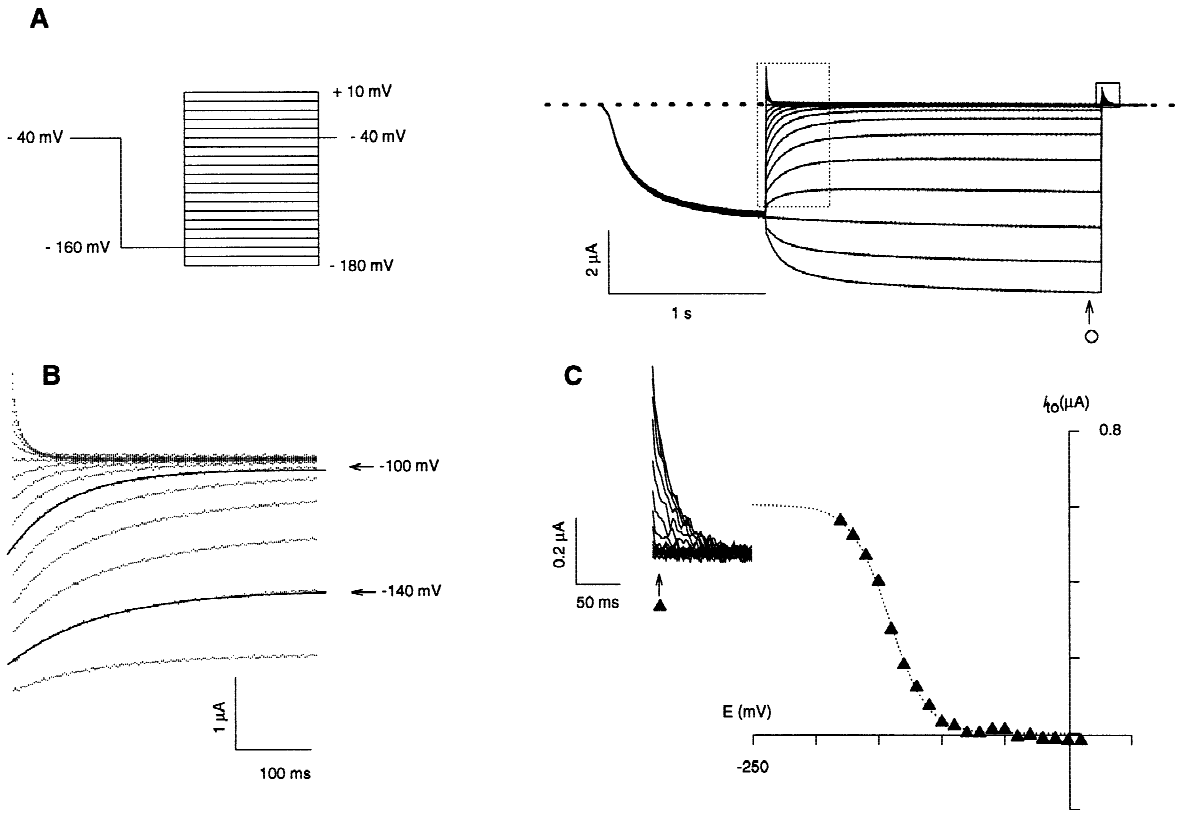

Fig. 1. Voltage and current traces recorded on KAT1-expressing oocytes. In this example, the bathing solution contained (in mM): 10 KCl, 90 NaCl, 1.8 $CaCl_2$, 1 $MgCl_2$, 5 HEPES, pH 7.4. (*A*) Voltage-clamp protocol (left, *see* text) and currents (right) recorded in an oocyte injected with 30 ng of KAT1 cRNA. The horizontal dashed line corresponds to zero currents. Steady-state currents were sampled (right upward arrow, open circle) at the end of the protocol for further analysis (*see* Fig. 2*B*). Deactivating currents (recorded after the activating prepulse at −160 mV: dotted frame) and so-called ''tail'' currents (deactivating currents when coming back to the holding potential: full-line frame) are shown with an expanded scale in (*B*) and (*C*, top) respectively. (*B*) Deactivating currents were fitted by a single exponential kinetics: the 2 lines (arrows) represent the fit of the current recorded at −140 and −100 mV. Initial values of this current obtained on each idealized trace were taken as the instantaneous KAT1 current and used to graphically determine the reversal potential of KAT1 current (*see* text). (*C*) Initial value of tail currents (i_{to}) was sampled 15 msec after the end of phase II (symbol and upward arrow in the top figure) and plotted against the voltage of the preceding pulse. The *I-V* relationship (bottom figure) was assumed to obey a two-state Boltzmann law (dotted curve, *see* text).

infinitely negative values of *E*, is asymptotic to a straight line crossing the origin of axes with a slope equal to G_l.

As previously shown by Hoshi (1995) and Véry et al. (1995), KAT1 behaves like a voltage-gated channel in which the open state probability is increased by hyperpolarization. It follows that, at finite negative values of *E*, the KAT1 macroscopic current *I* is only a fraction of I_{GHK} that can be approximated by a Boltzmann equation:

$$I = I_{GHK}/(1 + \exp(z_g \cdot A \cdot (E - E_{a50}))) \quad (5)$$

where E_{a50} is the half-activation potential and z_g is the equivalent gating charge (*Cf.*Hille, 1992). Finally, the following equation was used to simulate KAT1 steady-state current:

$$I = [G_l/(1 + \exp(z_g \cdot A \cdot (E - E_{a50})))] \cdot E \cdot [1 - \exp(A.(E - E_{rev}))]/[1 - \exp(A.E)] \quad (6)$$

where G_I, Z_g *et* E_{a50} are adjustable parameters. Adjustments are done by Marquardt-Levenberg algorithm (least square fitting).

Results

We used a double-pulse voltage-clamp protocol (Fig. 1*A*, left) consisting of 20 successive episodes. The holding potential was −40 mV, which is in the range of the resting potential of control oocytes and below the range of steady-state activation of KAT1 current (Véry et al., 1995). During the first pulse (duration 1 sec, phase I), the membrane potential was clamped to −160 mV (for all episodes). Then during the second pulse (duration 2 sec, phase II), the membrane potential was clamped to a value in the range of −180 mV to +10 mV (incremented by 10 mV between successive episodes). Typical current traces elicited by this voltage-clamp protocol are shown in Fig. 1*A* (right).

During phase I, a substantial fraction of KAT1 channels was activated. This allowed us to record, at the beginning of phase II, the peak current *i* flowing through

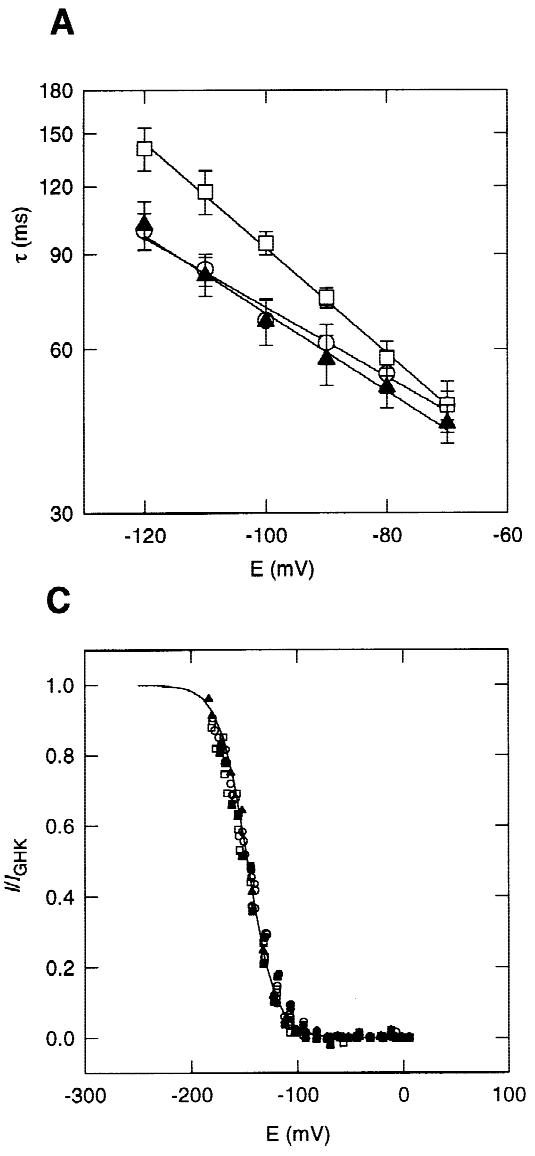

Fig. 2. Voltage-dependence of KAT1 deactivation time-constant, steady-state current and activation level in different bathing solutions. All solutions contained (in mM): 1.8 $CaCl_2$, 1 $MgCl_2$, 5 HEPES, pH 7.4 as a background, and 100 of either K^+ (open circle), Rb^+ (open square) or Na^+ (closed triangle) (the same symbols are used in *A*, *B* and *C*). (*A*) KAT1 deactivation time constant (τ). Values of τ were obtained by a single decaying exponential fit (least squares fitting) to KAT1 deactivating currents (*see* Fig. 1*B*). τ data are presented as mean ± SD ($n = 4$) with a logarithmic scale. The solid line is a linear fit to the data (*see* text). (*B*) KAT1 steady-state current. The symbols figure values of the steady-state KAT1 current, *I* (*see* Fig. 1*A*). The parameters of Eq. 6 (*see* Material and Methods) were adjusted to fit *I*. The full line and the dashed line curves show respectively the calculated voltage-dependence of *I* and I_{GHK} (which is the current predicted by the Goldman-Hodgkin-Katz theory). (*C*) KAT1 activation level at steady-state. A two-state Boltzmann relation (dotted line, *see* Eq. 6) modeled the I/I_{GHK} ratio. Symbols represent the data obtained from 4 different oocytes.

these channels at different potentials. The capacitance artifact was found to be complete after 15 msec, therefore values of *i* were sampled at 15 msec after the beginning of phase II. Data were plotted against membrane potential (*not shown*) to determine the reversal potential of the KAT1 current. When the phase II potential was more positive than the phase I potential, a decay of the *i* current was observed that could be fitted by a single exponential as shown in Fig. 1*B* (traces recorded at −140 and −100 mV).

During phase II, the transition from peak current (*i*) towards steady-state current (*I*) was recorded, and values of *I* were sampled at the end of phase II (symbol and upward arrow, Fig. 1*A* right). Plotting *I* data against membrane potential (Fig. 2*B*) showed the strong inward rectification of KAT1 channels, which was previously ascribed to voltage-gating (Hedrich et al., 1995; Hoshi, 1995; Véry et al., 1995). Here, this latter phenomenon was characterized by analyzing the deactivating currents recorded upon return to holding potential, after phase II. These tail currents (i_t, Fig. 1*C*, top) were found to decay exponentially with a time constant that was independent of the initial current amplitude (*not shown*). This initial value (i_{to}) depended strongly on the membrane potential during phase II (Fig. 1*C*, bottom). Data were fitted by a Boltzman equation ($i_{to} = i_{tomax}/[1 + \exp(z_g \cdot F \cdot (E - E_{a50})/R/T)]$, dotted curve); with values for the adjustable parameters of the model being $i_{tomax} = 603$ nA, $z_g = 1.74$ and $E_{a50} = -141.5$ mV.

Using the voltage-clamp protocol described above, we compared KAT1 currents recorded when bath solution was 100 mM RbCl or 100 mM KCl or 100 mM NaCl. As shown in Fig. 2*A*, τ increased exponentially with decreasing voltage from −80 to −120 mV in all 3 solu-

tions. While τ was approximately the same in all 3 solutions at −80 mV, τ was significantly higher in pure Rb^+ than in pure K^+ or pure Na^+ solution at −120 mV (Fig. 2*A*). Lower steady-state current was observed in pure Rb^+ (and much more lower in pure Na^+) than in pure K^+ solution (Fig. 2*B*). Analyzing the steady-state *I/V* plots (*see* Methods section) allowed us to derive limiting inward conductance values (G_l, slope of dotted lines at infinite negative voltage in Fig. 2*B*) and voltage-gating parameters of KAT1 channels (Fig. 2*C*). The ratio of G_l in pure Rb^+ solution to G_l in pure K^+ solution was 0.16 ± 0.03 ($n = 5$, Fig. 3*D;* 0.14 in the example shown in Fig. 2*B*). The ratio of G_l in pure Na^+ solution to G_l in pure K^+ solution was 0.019 ± 0.002 ($n = 3$, Fig. 3*D;* 0.017 in the example shown in Fig. 2*B*). These data are in agreement with previous reports (Schachtman et al., 1992; Uozumi et al., 1995; Véry et al., 1995). Gating parameters were not significantly different in pure Rb^+ ($z_g = 1.62 \pm 0.20$, $E_{a50} = -150 \pm 4$ mV, $n = 9$) or Na^+ ($z_g = 1.71 \pm 0.25$, $E_{a50} = -149 \pm 8$ mV, $n = 3$) from those in pure K^+ solution ($z_g = 1.53 \pm 0.23$, $E_{a50} = -1.47 \pm 5$ mV, $n = 9$). As previously shown and discussed in detail (Véry et al., 1995), these gating parameters, here derived from steady-state current analyses (Fig. 2*C*), are close to those derived from deactivating current analyses (Fig. 1*C*).

In further experiments we recorded KAT1 currents in mixtures of K^+ ions with either Na^+ or Rb^+ ions. In the following, data are expressed as a function of K^+/Na^+ or K^+/Rb^+ mole fraction (i.e., the ratio $[K^+]/([K^+] + [Rb^+])$ or $[K^+]/([K^+] + [Na^+])$, Figs. 3 and 4).

No AMFE was observed regarding the reversal potential, which varied according to the Goldman-Hodgkin-Katz model (Fig. 3*A*).

The τ value, which, in pure Na^+ solution was close to that in pure K^+ solution (Fig. 2*A*) showed little dependence on K^+/Na^+ mole fraction at any tested membrane potential (*see* Fig. 3*B*) for −120 mV and −80 mV, close and open squares resp.). A similar pattern was observed in K^+/Rb^+ mixtures at −80 mV (Fig. 3*B*, open circles). Conversely, upon hyperpolarizations in the −80 to −120 mV range, τ displayed increasingly non monotonic variation in function of the K^+/Rb^+ mole fraction (*see* close circles in Fig. 3*B* for −120 mV, condition of maximal variation of τ between pure K^+ and pure Rb^+ in Fig. 2*A*). The τ value reached a maximum for a ≈0.3 K^+/Rb^+ mole fraction. For up to 0.7 K^+/Rb^+ mole fractions, τ was closer to that in pure Rb^+ than to that in pure K^+ solution.

The value of I at −150 mV and the G_l estimate obtained in each tested K^+/Na^+ or K^+/Rb^+ mixture were compared to those in pure K^+ solution. The averaged data are plotted as relative current (i.e., relative chord conductance) or relative G_l against the K^+/Na^+ or K^+/Rb^+ mole fraction (Figs. 3*C* and *D*, resp.). Relative I and relative G_l displayed similar variations. They varied monotonically as a function of K^+/Na^+ mole fraction, but not with respect to the K^+/Rb^+ mole fraction (Figs. 3*C* and 3*D*, resp.). A minimum was reached for a K^+/Rb^+ mole fraction of ca. 0.25. It is worth noting that replacing 50 mM of the non-permeant Na^+ by 50 mM of the permeant Rb^+ decreased relative I and G_I values by 4 fold (50 mM K^+ was present in both cases, Figs. 3*C* and *D*).

Finally, we studied KAT1 mutants which were reported for an increased P_{Rb}/P_K relatively to the wild type (Becker et al., 1996). Accordingly, these mutants displayed a ca. 0.6 relative current (or relative G_I) in pure Rb^+ solution (Figs. 4*A* and *B*) much higher than the ca. 0.2 value obtained for the wild-type (Figs. 3*C* and *D*). In either of these mutants, a point mutation affect a threonine residue (T259 or T260) in the P domain. It is worth noting that T259 in the KAT1 P domain is at the same relative position than T441 in the Shaker P domain (Fig. 4*C*). Yool & Schwarz (1996) demonstrated that the single mutation T441S, which increases P_{NH4}/P_K (Yool & Schwarz, 1991), allowed an AMFE on reversal potential to be observed in mixtures of K^+ and NH_4^+. Both the T259S and T260S mutants on KAT1 displayed AMFE on relative I and relative G_l which were more pronounced than those displayed by the wild-type (compare Figs. 4A and 4B to Figs. 3C and 3D); however, no AMFE on reversal potential could be seen (*data not shown*).

Discussion

The ability of Rb^+ ions to carry current through the K^+-selective channel KAT1 (Fig. 2*B*) allowed us to search for anomalous mole fraction effects (AMFE) in mixtures of K^+ and Rb^+. Also, parallel experiments were performed in mixtures with K^+ and the non-permeant Na^+ ion (Fig. 2*B*).

Compared to K^+, Rb^+ decreased the KAT1 deactivation rate while Na^+ did not (Figs. 2*A* and 3*B*). Interactions between permeant ions and channel gating were first reported in acetylcholine receptor channels (Van Helden, Hamill & Gage, 1977; Ascher, Marty & Neild, 1978), and then in several kinds of K^+ channels (Hagiwara & Yoshii, 1979; Swenson & Armstrong, 1981; Cahalan et al., 1985; Matteson & Swenson, 1986; Hu, Yamamoto & Kao, 1989; Spruce, Standen & Stanfield, 1989; Demo & Yellen, 1992; Clay, 1996), and Ca^{2+} channels (Eckert & Chad, 1984; Nelson, French & Krueger, 1984; Chesnoy-Marchais, 1985). A voltage-dependent effect of Rb^+ on τ (Fig. 2*A*) is believed to involve an interacting site which should be located within the membrane electric field (Matteson & Swenson, 1986; Sala & Matteson, 1991). This is known as the 'foot in the door effect' or 'occupancy hypothesis' (Yeh & Armstrong, 1978; Swenson & Armstrong, 1981). It is

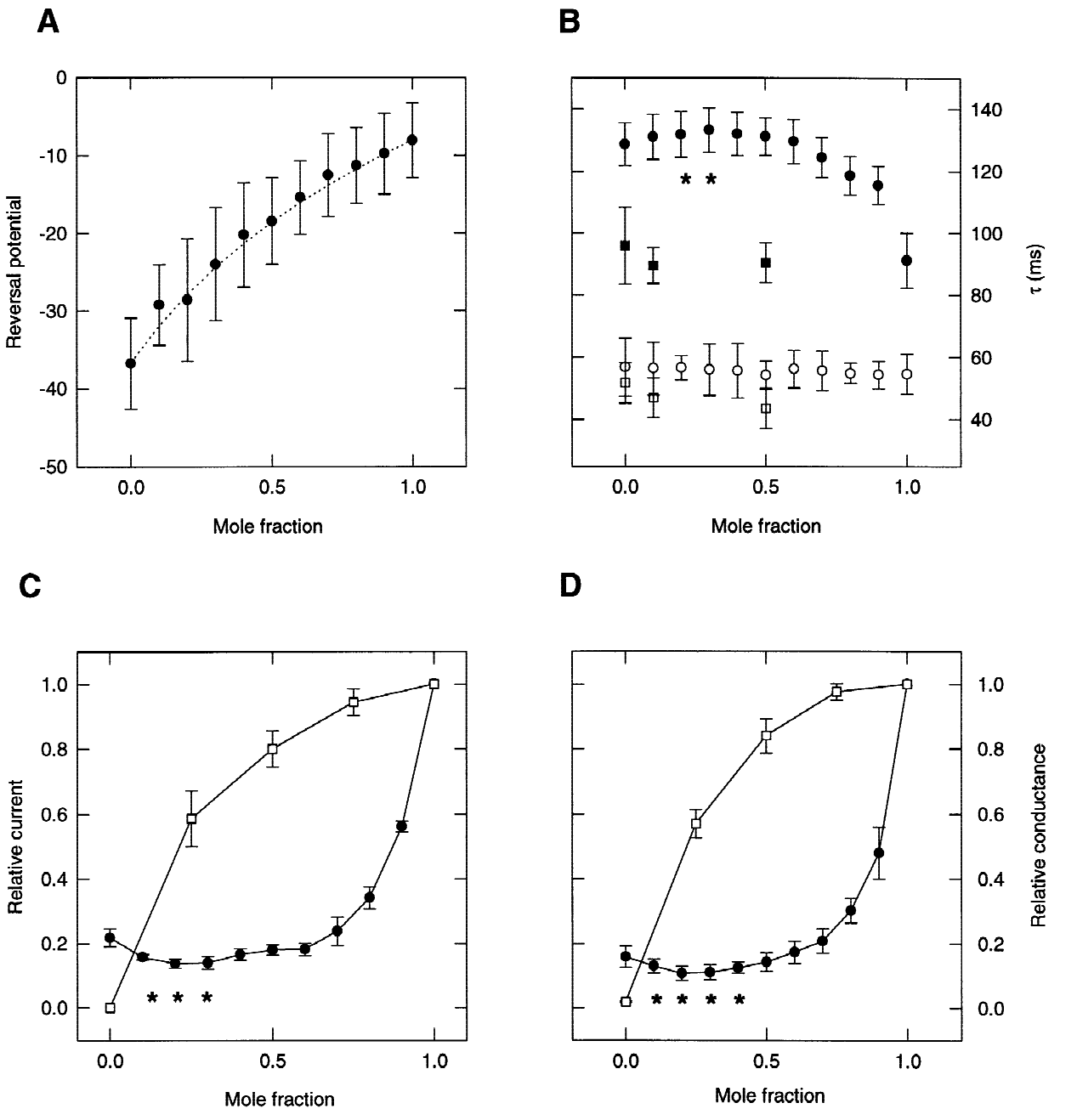

Fig. 3. Effect of K^+/Rb^+ and K^+/Na^+ mole fraction on some KAT1 features. KAT1 currents were recorded in oocytes perfused by solutions containing a total monovalent cation concentration of 100 mM with different proportions of K^+ and Na^+ (square) or K^+ and Rb^+ (circle). Ionic conditions were tested in series on the same oocyte. Results are presented as mean ± SD ($n = 4$ oocytes). (*A*) Dependence of reversal potential (E_{rev}) of KAT1 current on K^+/Rb^+ mole fraction. E_{rev} values were obtained as described in Fig. 1*B*. The symbols represent the data as mean ± SD ($n = 4$ oocytes). The dashed line corresponds to $E_{rev} = (R \cdot T/F)$. $ln[(Rb_e^+ \cdot P_{Rb}/P_K + K_e^+)/K_i^+]$, using parameters as follows: Rb_e^+ and K_e^+ were respectively Rb^+ and K^+ external concentration; K_i^+ was the internal K^+ concentration, calculated as $K_i^+ = 100 \cdot \exp(-E_{revK100} \cdot F/(R \cdot T))$ (in mM, $E_{revK100}$ being E_{rev} in 100 mM KCl solution); P_{Rb}/P_K was the Rb^+ *vs.* K^+ permeability ratio, calculated as $P_{Rb}/P_K = \exp[(E_{revRb100} - E_{revK100}) \cdot F/(R \cdot T)]$. (*B*) Dependence of KAT1 deactivating time constant (τ) on K^+/Na^+ and K^+/Rb^+ mole fraction. τ values were obtained as in Fig. 2*A* at either −80 mV (open symbols) or −120 mV (closed symbols). (*C*) Dependence of KAT1 current on K^+/Na^+ and K^+/Rb^+ mole fraction. The 'relative current' is the ratio between the current at −150 mV at a given mole fraction and that measured in pure K^+ solution. (*D*) Dependence of KAT1 conductance on K^+/Na^+ and K^+/Rb^+ mole fraction. The 'relative conductance' is the ratio between the limit inward conductance (*see* Materials and Methods) calculated at a given mole fraction and that calculated in pure K^+ solution. The data marked by * in (*C*) and (*D*) are significantly different than the value obtained in 0.0 mole fraction solution at $P < 0.01$ (Student's *t* test).

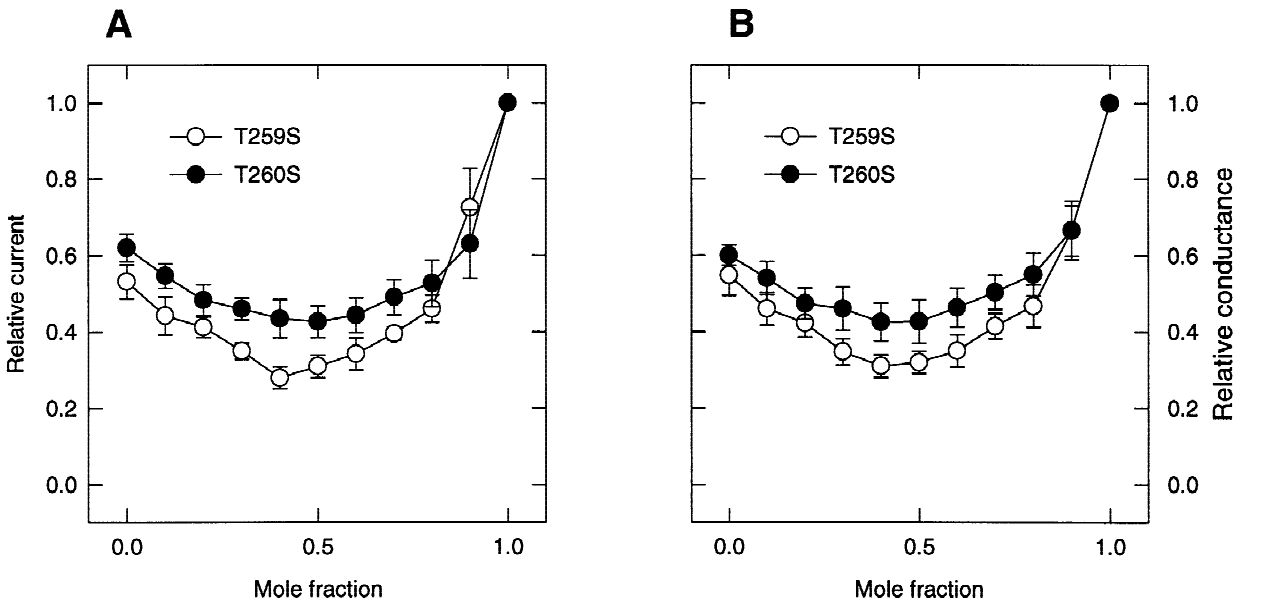

C

```
                                    **
KAT1:    248-272 VTALYWSITTLTTTGYGDFHAENPR
Shaker:  430-454 PDAFWWAVVTMTTVGYGDMTPVGFW
                                    *
```

Fig. 4. Effect of K^+/Rb^+ and K^+/Na^+ mole fraction on conductance of KAT1 pore mutants. Currents were recorded in oocytes perfused by solutions containing a total monovalent cation concentration of 100 mM with different proportions K^+ and Rb^+. Ionic conditions were tested in series on the same oocyte. Results are presented as mean ± SD ($n = 4$ oocytes). (*A*) Dependence of current through KAT1 pore mutants on K^+/Rb^+ mole fraction. The 'relative current' is the ratio between the current at −150 mV at a given mole fraction and that measured in pure K^+ solution. (*B*) Dependence of conductance of KAT1 pore mutants on K^+/Rb^+ mole fraction. The 'relative conductance' is the ratio between the limit inward conductance (*see* Materials and Methods) calculated at a given mole fraction and that calculated in pure K^+ solution. (*C*) Alignment of amino-acid sequences of the pore regions (GYGD in boldface) of KAT1 (Anderson et al., 1992) and Shaker-A (Tempel et al., 1987). Stars indicate the KAT1 mutants (T259S and T260S; Becker et al., 1996) presently studied, and the ShA mutant (T441S) studied by Yool & Schwarz (1996).

assumed that when an ion is present in the pore, it prevents channel closing, thus increasing the mean open time (Spruce et al., 1989; Demo & Yellen, 1992) and slowing the deactivation rate of macroscopic current (Matteson & Swenson, 1986; Sala & Matteson, 1991). It is therefore expected that the more tightly an ion interacts with the pore, the more the deactivation is slowed. In this framework, taking K^+ as reference, the slowing effect of Rb^+ on the deactivation of KAT1 may originate from higher affinity binding or longer residence within the pore of Rb^+. On the contrary, as KAT1 deactivation rate was essentially independent of the K^+/Na^+ mole fraction (Fig. 3*B*), it can be assumed that Na^+ either does not enter the pore or binds to it no more tightly than K^+.

Although the mean relative permeability coefficient P_{Rb}/P_K (derived from reversal potential) is close to 0.35, the mean relative conductance G_{Rb}/G_K is only 0.2 (Figs. 2*B*, 3C and D). Similar findings regarding a Ca^{2+}-activated K^+ channel (Hu et al., 1989) and a ATP-blockable K^+ channel (Ashcroft, Kakei & Kelly, 1989) led to suggest that Rb^+ binds more tightly to the pore than does K^+. For KAT1 channel, this hypothesis is further supported by the inhibition of K^+ current by Rb^+ (Fig. 3*C*).

A K^+/Rb^+ AMFE is shown on KAT1 deactivation rate in Fig. 3*B*. The fact that τ in K^+/Rb^+ mixtures was close to τ in pure Rb^+ suggests that most KAT1 channels were occupied by Rb^+ ions. It is therefore expected that in K^+/Rb^+ mixtures the KAT1 conductance was mainly due to Rb^+ (*see below*). To our knowledge such an AMFE on channel deactivation rate has not been previously reported.

AMFE on channel conductance is usually described from single channel recordings. KAT1 single channel conductance, however, was shown to be only 5 pS in symmetrical 100 to 150 mM K^+ (Hoshi, 1995; Hedrich et

al., 1995). From the data on macroscopic KAT1 current (Fig. 2*B*), it can be assumed that, in pure symmetrical Rb^+, KAT1 single channel conductance would fall in the 1 pS range, and even less in some K^+/Rb^+ mixtures. Therefore, we preferred to investigate AMFE on KAT1 conductance by analyzing the macroscopic current. A simple method was the comparison of steady-state current recorded at a given potential (i.e., plotting chord conductance *vs.* mole fraction, *see* Figs. 3*C* and 4*A*). In the case of voltage-gated channels, the gating may depend on ionic conditions or on point mutations, so chord conductance analyses may be misleading. Therefore, we made parallel analyses on the so-called macroscopic 'limit inward conductance' (G_l, Figs. 3*D* and 4*B*).

G_l values were derived from analyzing data with the help of the Goldman-Hodgkin-Katz model. In this model, interactions between a given ion and the channel are crudely viewed as friction: this is expressed by the P_X coefficients (Eqs. 1 to 4), which are expected to be constants, independent of the concentration of their related ion and also of other ions. The GHK model was often reported to predict satisfactorily current-voltage relations in K^+ channels provided that *ad hoc* values of P_K were considered for different ionic concentrations (e.g., Goldstein et al., 1996; Duprat et al., 1997; Leonoudakis et al., 1998). Therefore, in given ionic conditions (when E in equations (1) to (4) is the only variable), the relationship of current to voltage predicted by the GHK model was, in practice, reliable. For example, Duprat et al. (1997) proposed that *ad hoc* values of P_K corresponded to a constant permeability coefficient scaled by a factor to take account of the sensitivity of conductance to external K^+. In our analyses, the G_l parameter concatenates ion concentrations and *ad hoc* permeability coefficients. The agreement between voltage-gating parameters (z_g and E_{a50}) obtained by this method (Fig. 2*C*) and those obtained independently by analyzing deactivating currents (Fig. 1*C*) validates *a posteriori* the use of the above Eq. 6.

We did not observe an AMFE on reversal potential in mixtures of K^+ and Rb^+ (Fig. 3*A*). A similar absence of effect has been described for the Shaker H4 channel (Heginbotham & MacKinnon, 1993) which displays an AMFE for single channel conductance but not for reversal potential of macroscopic current. The K^+/Rb^+ AMFE on KAT1 channel conductance shown in Figs. 3*C* and *D*, as well as in the KAT1 pore mutants (Fig. 4), strongly supports the multi-ion nature of this channel. The slowly permeating Rb^+ ion therefore behaves as a permeant blocker of KAT1 channel.

With some exceptions (*see* Introduction), the models which have been discussed in the literature to explain the AMFE share two main assumptions: first, several ions can occupy the pore at the same time (i.e., 'multi-ion pore behavior') and second, these ions go through the pore in single file. During their progress through the pore, ions interact successively with one or several sites. It is believed that at least one energy barrier cannot be passed by an ion without some interaction involving another ion within the pore. Anomalous mole fraction effects are thought to originate from the different efficiencies of various permeant species in relieving a neighboring ion.

Without deriving a quantitative energy barrier model for the KAT1 pore, the following conduction scheme can be proposed to provide a qualitative understanding of the AMFE discussed above. In pure K^+ solution, the weak interactions between ions and the pore allow the maximum KAT1 conductance, whereas in pure Rb^+ solutions, conductance is decreased because Rb^+ interacts more tightly than K^+ with the pore. In low K^+/Rb^+ mole fraction solutions, an open channel is more likely to be penetrated first by a Rb^+ ion. It is observed, at least in some low K^+/Rb^+ mole fraction solutions, that conductance can be less than in pure Rb^+ solution. In such cases, once a Rb^+ ion is bound to the pore, it is assumed that it can be much more easily relieved (and freed in the inner mouth of the pore) if the second penetrating ion is another Rb^+ than if it is a K^+. Our present data on KAT1 suggest that this phenomenon would be worsened in both T259S and T260S mutants compared to the wild type.

Sharing not only structural homologies with the predicted structure of the Shaker channel, KAT1 displays permeation properties which are similar to those of animal members of the Shaker superfamily: selective permeability to K^+ over Rb^+, anomalous mole fraction effects on conductance, and ionic influences on deactivation rates. However, the KAT1 channel also displays unique features: it rectifies inwardly, it does not inactivate and enables slowly activating currents, which can be easily studied in oocytes. Furthermore, as KAT1 can complement yeast (*Saccharomyces cerevisiae*) strains defective in K^+ uptake, mutants of interest can easily be screened by phenotype (Uozumi et al., 1995; Becker et al., 1996). The present paper is the first report of evidence for a multi-ion conducting scheme for KAT1, supporting the view that this channel is an interesting model for studies on ionic interaction with permeation and gating mechanisms.

Dr. D. Becker and Prof. R. Hedrich (University of Würzburg, Germany) kindly provided the KAT1 mutants. We are very grateful to Dr. J. Neyton (ENS/CNRS, Paris, France) and Dr. A. Yool (University of Arizona, Tucson, AZ) for helpful discussions and Dr. S. Staunton (INRA Montpellier) for English corrections. We thank Dr. X. Sarda for help with cRNA preparation. B. Lacombe was funded by the INRA.

Note Added in Proof

During the reviewing process, KAT1 was demonstrated to be a multi-ion channel by another experimental approach (Moroni, A., Bardella, L., Thiel, G. 1998. The

impermeant ion methylammonium blocks K^+ and NH_4^+ currents through KAT1 channel differentially: evidence for ion interaction in channel permeation. *J Membrane Biol.* **163:**25–35)

References

Aidley, D.J., Stanfield, P.R. 1996. Ion Channels: Molecules in Action. Cambridge University Press, Cambridge, UK

Anderson, J.A., Huprikar, S.S., Kochian, L.V., Lucas, W.J., Gaber, R.F. 1992. Functional expression of a probable *Arabidopsis thaliana* potassium channel in *Saccharomyces cerevisiae*. *Proc. Natl. Acad. Sci. USA* **89:**3736–3740

Armstrong, C.M., Neyton, J. 1992. Ion permeation through calcium channels: a one-site model. *Ann. N.Y. Acad. Sci.* **635:**18–25

Ascher, P., Marty, A., Neild, T.O. 1978. Lifetime and elementary conductance of the channels mediating the excitatory effects of acetylcholine in *Aplysia* neurons. *J. Physiol.* **278:**177–206

Ashcroft, F.M., Kakei, M., Kelly, R.P. 1989. Rubidium and sodium permeability of the ATP-sensitive K^+ channel in single rat pancreatic β-cells. *J. Physiol.* **408:**413–430

Becker, D., Dreyer, I., Hoth, S., Reid, J.D., Busch, H., Lehnen, M., Palme, K., Hedrich, R. 1996. Changes in voltage activation, Cs^+ sensitivity, and ion permeability in H5 mutants of the plant K^+ channel KAT1. *Proc. Natl. Acad. Sci. USA* **93:**8123–8128

Begenisich, T., Smith, C. 1984. Multi-ion nature of potassium channels in squid axons. *Curr. Top. Membr. Transp.* **22:**353–369

Bertl, A., Anderson, J.A., Slayman, C.L., Gaber, R.F. 1995. Use of *Saccharomyces cerevisiae* for patch clamp analysis of heterologous membrane proteins: characterization of Kat1, an inward-rectifying K^+ channel from *Arabidopsis thaliana*, and comparison with endogenous yeast channels and carriers. *Proc. Natl. Acad. Sci. USA* **92:**2701–2705

Cahalan, M.D., Begenisich, T.B. 1976. Sodium channel selectivity: dependence of internal permeant ion concentration. *J. Gen. Physiol.* **68:**11–125

Cahalan, M.D., Chandy, K.G., DeCoursey, T.T., Gupta, S. 1985. A voltage-gated potassium channel in human T lymphocytes. *J. Physiol.* **358:**197–237

Campbell, D.L., Rasmusson, R.L., Strauss, H.C. 1988. Theoretical study of the voltage and concentration dependence of the anomalous mole fraction effect in single calcium channels. *Biophys. J.* **54:**945–954

Chérel, I., Daram, P., Gaymard, F., Horeau, C., Thibaud, J.-B., Sentenac, H. 1996. Plant potassium channels: structure, activity and function. *Biochem. Soc. Trans.* **24:**964–971

Chesnoy-Marchais, D. 1985. Kinetic properties and selectivity of calcium-permeable single channels in *Aplysia* neurons. *J. Physiol.* **367:**457–488

Clay, J.R. 1996. Effects of permeant cations on K^+ channel gating in nerve axons revisited. *J. Membrane Biol.* **153:**195–201

Dang, T.X., McCleskey, E.W. 1998. Ion channel selectivity through stepwise changes in binding affinity. *J. Gen. Physiol.* **111:**185–193

Daram, P., Urbach, S., Gaymard, F., Sentenac, H., Chérel, I. 1997. Tetramerization of the AKT1 plant potassium channel involves its C-terminal cytoplasmic domain. *EMBO J* **16:**3455–3463

Demo, S.D., Yellen, G. 1992. Ion effects on gating of the Ca^{2+}-activated K^+ channel correlate with occupancy of the pore. *Biophys. J.* **61:**639–648

DiFrancesco, D., Ferroni, A., Mazzanti, M., Tromba, C. 1986. Properties of the hyperpolarization-activated current (i_f) in cells isolated from the rabbit sino-atrial node. *J. Physiol.* **377:**61–88

Doyle, D.A., Morais Cabral, J., Pfuetzner, R.A., Kuo, A., Gulbis, J.M., Cohen, S.L., Chait, B.T., MacKinnon, R. 1998. The structure of the potassium channel: molecular basis of K^+ conduction and selectivity. *Science* **280:**69–77

Draber, S., Schultze, R., Hansen, U.P. 1991. Patch-clamp studies on the anomalous mole fraction effect of the K^+ channel in the cytoplasmic droplets of *Nitella:* an attempt to distinguish between a multi-ion single-file pore and an enzyme kinetic model with lazy state. *J. Membrane Biol.* **123:**183–190

Dreyer, I., Antunes, S., Hoshi, T., Müller-Rober, B., Palme, K., Pongs, O., Reintanz, B., Hedrich, R. 1997. Plant K^+ channel α-subunits assemble indiscriminately. *Biophys. J.* **72:**2143–2150

Duprat, F., Lesage, F., Fink, M., Reyes, R., Heurteaux, C., Lazdunski, M. 1997. TASK, a human background K^+ channel to sense external pH variations near physiological pH. *EMBO J.* **16:**5464–5471

Eckert, R., Chad, J.E. 1984. Inactivation of calcium channels. *Prog. Biophys.* **44:**215–267

Eisenman, G., Latorre, R., Miller, C. 1986. Multi-ion conduction and selectivity in the high-conductance Ca^{++}-activated K^+ channel from skeletal muscle. *Biophys. J.* **50:**1025–1034

Friel, D.D., Tsien, R.W. 1989. Voltage-gated calcium channels: direct observation of the anomalous mole fraction effect at the single-channel level. *Proc. Natl. Acad. Sci. USA* **86:**5207–5211

Goldstein, S.A.N., Price, L.A., Rosenthal, D.N., Pausch, M.H. 1996. ORK1, a potassium-selective leak channel with two pore domains cloned from *Drosophila melanogaster* by expression in *Saccharomyces cerevisiae*. *Proc. Natl. Acad. Sci. USA* **93:**13256–13261

Hagiwara, S., Takahashi, K. 1974. The anomalous rectification and cation selectivity of the membrane of a starfish egg cell. *J. Membrane Biol.* **18:**61–80

Hagiwara, S., Yoshii, M. 1979. Effects of internal potassium and sodium on the anomalous rectification of the starfish egg as examined by internal perfusion. *J. Physiol.* **292:**251–265

Hagiwara, S., Miyazaki, S., Krasne, S., Ciani, S. 1977. Anomalous permeabilities of the egg cell membrane of a starfish in K^+-Tl^+ mixtures. *J. Gen. Physiol.* **70:**269–281

Hedrich, R., Moran, O., Conti, F., Busch, H., Becker, D., Gambale, F., Dreyer, I., Küch, A., Neuwinger, K., Palme, K. 1995. Inward rectifier potassium channels in plants differ from their animal counterparts in response to voltage and channel modulators. *Eur. Biophys. J.* **24:**107–115

Heginbotham, L., MacKinnon, R. 1993. Conduction properties of the cloned *Shaker* K^+ channel. *Biophys. J.* **65:**2089–2096

Hess, P., Tsien, R.W. 1984. Mechanism of ion permeation through calcium channels. *Nature* **309:**453–456

Hille, B. 1975. Ionic selectivity, saturation, and block in sodium channels: a four-barrier model. *J. Gen. Physiol.* **66:**535–560

Hille, B. 1992. Ionic Channels of Excitable Membranes. 2nd Ed., Sinauer Associates, Sunderland, MA

Hille, B., Schwarz, W. 1978. Potassium channels as multi-ion single file pores. *J. Gen. Physiol.* **72:**409–442

Hodgkin, A.L., Huxley, A.F. 1952. Currents carried by sodium and potassium through the membrane of the giant axon of *Loligo*. *J. Physiol.* **116:**449–472

Hoshi, T. 1995. Regulation of voltage dependence of the KAT1 channel by intracellular factors. *J. Gen. Physiol.* **105:**309–328

Hu, S.L., Yamamoto, Y., Kao, C.Y. 1989. Permeation, selectivity and blockade of the Ca^{2+}-activated potassium channel of the guinea pig taenia coli myocyte. *J. Gen. Physiol.* **94:**849–862

Jan, L.Y., Jan, Y.N. 1997. Cloned potassium channels from eukaryotes and prokaryotes. *Annu. Rev. Neurosci.* **20:**91–123

Kiss, L., Immke, D., LoTurco, J., Korn, S.J. 1998. The interaction of Na^+ and K^+ in voltage-gated potassium channels: evidence for cation binding sites of different affinity. *J. Gen. Physiol.* **111:**195–206

Leonoudakis, D., Gray, A.T., Winegar, B.D., Kindler, C.H., Harada, M., Taylor, D.M., Chavez, R.A., Forsayeth, J.R., Yost, C.S. 1998. An open rectifier potassium channel with two pore domains in tandem from rat cerebellum. *J. Neurosci.* **18:**868–877

Lester, H.A., Dougherty, D.A. 1998. New views of multi-ion channels. *J. Gen. Physiol.* **111:**181–183

Marten, I., Gaymard, F., Lemaillet, G., Thibaud, J.-B., Sentenac, H., Hedrich, R. 1996. Functional expression of the plant K^+ channel KAT1 in insect cells. *FEBS Lett.* **380:**229–232

Matteson, D.R., Swenson, R.P. 1986. External monovalent cations that impede the closing of K channels. *J. Gen. Physiol.* **87:**795–816

Mayer, M.L., Westbrook, G.L. 1983. A voltage-clamp analysis of inward (anomalous) rectification in mouse spinal sensory ganglion neurones. *J. Physiol.* **340:**19–45

McCormick, D.A., Pape, H. 1990. Properties of a hyperpolarization-activated cation current and its role in rhythmic oscillation in thalamic relay neurones. *J. Physiol.* **431:**291–318

Mienville, J.M., Clay, J.R. 1997. Ion conductance of the Ca-activated maxi-K channel from the embryonic rat brain. *Biophys. J.* **72:**188–192

Miller, C. 1996. The long pore gets molecular. *J. Gen. Physiol.* **107:**445–447

Mironov, S.L. 1992. Conformational model for ion permeation in membrane channels: a comparison with multi-ion models and applications to calcium channel permeability. *Biophys. J.* **63:**485–496

Nelson, M.T., French, R.J., Krueger, B.K. 1984. Voltage-dependent calcium channels from brain incorporated into planar lipid bilayers. *Nature* **308:**77–80

Nonner, W., Chen, D.P., Eisenberg, B. 1998. Anomalous mole fraction effect, electrostatics, and binding in ionic channels. *Biophys. J.* **74:**2327–2334

Pérez-Cornejo, P., Begenisich, T. 1994. The multi-ion nature of the pore in *Shaker* K^+ channels. *Biophys. J.* **66:**1929–1938

Sala, S., Matteson, D.R. 1991. Voltage-dependent slowing of K channel closing kinetics by Rb^+. *J. Gen. Physiol.* **98:**535–554

Santoro, B., Grant, S.G.N., Bartsch, D., Kandel, E.R. 1997. Interactive cloning with the SH3 domain of N-src identifies a new brain specific ion channel protein, with homology with eag and cyclic nucleotide-gated channels. *Proc. Natl. Acad. Sci. USA* **94:**14815–14820

Santoro, B., Liu, D.T., Yao, H., Bartsch, D., Kandel, E.R., Siegelbaum, S.A., Tibbs, G.R. 1998. Identification of a gene encoding a hyperpolarization-activated pacemaker channel of brain. *Cell* **93:**717–729

Schachtman, D.P., Schroeder, J.I., Lucas, W.J., Anderson, J.A., Gaber, R.F. 1992. Expression of an inward-rectifying potassium channel by the *Arabidopsis* KAT1 cDNA. *Science* **258:**1654–1658

Schroeder, J.I., Ward, J.M., Gassman, W. 1994. Perspective on the physiology and structure of inward-rectifying K^+ channels in higher plants: biophysical implication for K^+ uptake. *Annu. Rev. Biophys. Biomol. Struct.* **23:**441–471

Shumaker, M.F., MacKinnon, R. 1990. A simple model for multi-ion permeation: single-vacancy conduction in a simple pore model. *Biophys. J.* **58:**975–984

Spruce, A.E., Standen, N.B., Stanfield, P.R. 1989. Rubidium ions and the gating of delayed rectifier potassium channels of frog skeletal muscle. *J. Physiol.* **411:**597–610

Stampe, P., Begenisich, T. 1996. Unidirectional K^+ fluxes through recombinant *Shaker* potassium channels expressed in single *Xenopus* oocytes. *J. Gen. Physiol.* **107:**449–457

Swenson, R.P., Armstrong, C.M. 1981. K^+ channels close more slowly in the presence of external K^+ and Rb^+. *Nature* **291:**427–429

Tabcharani, J.A., Rommens, J.M., Hou, Y.X., Chang, X.B., Tsui, L.C., Riordan, J.R., Hanrahan, J.W. 1993. Multi-ion pore behavior in the CFTR chloride channel. *Nature* **366:**79–82

Tester, M. 1988. Potassium channels in the plasmalemma of *Chara corallina* are multi-ion pores: voltage-dependent blockade by Cs^+ and anomalous permeabilities. *J. Membrane Biol.* **105:**87–94

Tempel, B.L., Papazian, D.M., Schwarz, T.L., Jan, Y.N., Jan, L.Y. 1987. Sequence of a probable potassium channel component encoded at *Shaker* locus of *Drosophila*. *Science* **237:**770–774

Uozumi, N., Gassman, W., Cao, Y., Schroeder, J.I. 1995. Identification of strong modifications in cation selectivity in an *Arabidopsis* inward rectifying potassium channel by mutant selection in yeast. *J. Biol. Chem.* **41:**24276–24281

Van Helden, D., Hamill, O.E., Gage, P.W. 1977. Permeant ions alter endplate channel characteristics. *Nature* **269:**711–712

Véry, A.-A., Bosseux, C., Gaymard, F., Sentenac, H., Thibaud, J.-B. 1994. Level of expression in *Xenopus* oocytes affects some characteristics of a plant inward-rectifying voltage-gated K^+ channel. *Pfluegers Arch.* **428:**422–424

Véry, A.-A., Gaymard, F., Bosseux, C., Sentenac, H., Thibaud, J.-B. 1995. Expression of a cloned plant K^+ channel in *Xenopus* oocytes: analysis of macroscopic currents. *Plant J.* **7:**321–332

Wagoner, P.K., Oxford, G.S. 1987. Cation permeation through the voltage-dependent potassium channel in the squid axon: characteristics and mechanisms. *J. Gen. Physiol.* **90:**261–290

Wollmuth, L.P. 1995. Multiple ion binding sites in I_h channels of rod photoreceptors from tiger salamanders. *Pfluegers Arch.* **430:**34–43

Woodhull, A.M. 1973. Ionic blockage of sodium channels in nerve. *J. Gen. Physiol.* **61:**687–708

Yang, J., Ellinor, P.T., Sather, W.A., Zhang, J.F., Tsien, R.W. 1993. Molecular determinants of Ca^{2+} selectivity and ion permeation in L-type Ca^{2+} channels. *Nature* **366:**158–161

Yeh, J.Z., Armstrong, C.M. 1978. Immobilization of gating charge by a substance that stimulates inactivation. *Nature* **273:**387–389

Yool, A.J., Schwarz, T.L. 1991. Alteration of ionic selectivity of a K^+ channel by mutation of the H5 region. *Nature* **349:**700–704

Yool, A.J., Schwarz, T.L. 1996. Anomalous mole fraction effect induced by mutation of the H5 pore region in the *Shaker* K^+ channel. *Biophys. J.* **71:**2467–2472